

Low energy deuteron-induced reactions on ^{27}Al and ^{56}Fe

S. I. Al-Quraishi,* C. E. Brient, S. M. Grimes, T. N. Massey, J. Oldendick, and R. Wheeler
Ohio University, Athens, Ohio 45701

(Received 23 November 1999; published 20 September 2000)

Measurements of the elastic and inelastic scattering cross sections for deuterons on ^{27}Al and ^{56}Fe have been completed at 5 and 7 MeV. Additional measurements of the (d,p) , (d,α) , and (d,n) spectra on these targets at the same energies have been made. An optical model analysis has yielded optical parameters for these nuclei. These are not consistent with some global models based on fits to data above 9 MeV. A Hauser-Feshbach calculation for each target at the appropriate bombarding energy has been compared with the various particle spectra. Evidence for both direct and compound nuclear reaction contributions is found. A small contribution is found from direct three-body breakup ($d+T\rightarrow n+p+T$), but (d,n) and (d,p) direct reactions to bound states are more common. Approximately 75% of the absorption cross section corresponds to compound nuclear processes.

PACS number(s): 25.45.De, 25.45.Hi

I. INTRODUCTION

Deuteron-induced reactions can be complex even at low energies because of the composite nature of the projectile. Proton or neutron projectiles with energies less than 8 MeV typically produce reactions with only one outgoing particle. The very small binding energy of the deuteron (2.2 MeV) allows a variety of reactions to occur at low bombarding energy. Most studies of deuteron-induced reactions at low bombarding energies have studied (d,p) or (d,n) cross sections to look for single-particle strength or have analyzed the excitation functions with compound nuclear models. Studies of the elastic scattering have been made by different groups and no effort has been made to do a comprehensive study.

The present experiment was undertaken in order to provide information on all reaction channels energetically available to deuteron-induced reactions on targets of ^{27}Al and ^{56}Fe . Cross sections for elastic and inelastic scattering of deuterons as well as for (d,p) , (d,n) , and (d,α) reactions were measured. The spectrometer used was capable of seeing ^3He and ^3H particles as well, but these channels had cross sections which were too small to be measured.

A special effort was made to cover the widest possible range of outgoing particle energies. The complicating aspect of this are the very different $\Delta E/\Delta x$ values for the various charged ejectiles. It was clear that a conventional $E-\Delta E$ telescope would have been rather limiting. Thus, a time-of-flight charged-particle spectrometer was developed. This instrument uses a single detector to obtain an energy signal and a time of flight. With both of these parameters available, the mass of the particle can be inferred.

Similarly, an effort was made to obtain the neutron spectrum over as broad a range as possible. Typically, NE213 detectors are used as neutron detectors because of their excellent timing and pulse-shape-discrimination capability. These detectors usually have difficulty detecting neutrons with energies less than 400 keV. Lithium-loaded glass scin-

tillators were chosen instead. These respond to neutrons of essentially zero energy and up and allow the entire spectrum to be obtained.

II. MEASUREMENTS AND ANALYSIS

Beams of 5 and 7 MeV deuterons were obtained from the John E. Edwards Laboratory Tandem Van de Graaff at Ohio University. Charged-particle spectra were accumulated for all outgoing charged-particle species simultaneously, while the neutron spectra were obtained in a separate measurement.

The charged-particle spectrometer utilized a 1.7 m flight path and a 1500 μ silicon-surface-barrier detector. A burst width of about 2 ns was obtained for the deuteron beam. Clean separation between particles of mass 1, 2, and 4 was obtained; mass 3 particles could have been observed but appear to have cross sections too small to measure in this energy region. This conclusion is not surprising since the thresholds for (d,t) and $(d,^3\text{He})$ are close to the 7 MeV bombarding energy.

Cross sections for protons, deuterons and alpha particles were measured at 10° intervals between 10° and 140° . A monitor detector was placed at 90° . Background measurements were taken with carbon and oxygen targets. The contribution to the various emission spectra from these contaminants was subtracted from the measurements using the elastic scattering peaks to obtain the normalization.

A further advantage of measuring carbon and oxygen spectra was that the larger change in outgoing energy with angle allowed an accurate angle calibration for each spectrometer setting. The angle could be set to an accuracy of $\pm 0.3^\circ$, but the use of the impurity peaks allowed this to be reduced to $\pm 0.1^\circ$.

Charged particle spectra were separated into energy spectra for various masses by setting mass windows on the two-dimensional time-of-flight versus energy plots. Typical spectra are shown in Figs. 1 and 2. The positive Q for (d,p) and (d,α) reactions allow a wide energy range of outgoing particles to be produced. For the (d,d') reaction, relatively few states were observed and the angle integrated (d,d') cross sections summed over all final states were less than 2% of

*Present address: King Fahd University of Petroleum and Minerals, Physics Department, Dhahran 31261, Saudi Arabia.

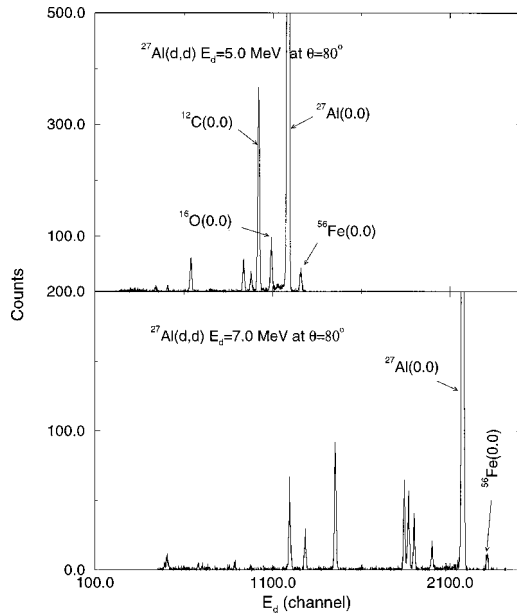


FIG. 1. Typical deuteron spectra. The data shown are for $^{27}\text{Al}(d,d)$ and $^{27}\text{Al}(d,d')$ at 80° .

the nonelastic cross section for both targets and both bombarding energies.

Neutron spectra were measured using the beam swinger facility of the Edwards Laboratory. Four lithium-loaded glass detectors were used at a flight path of 10 m to determine the neutron spectrum. The time calibration of the spectrum was done in two steps. A “random” spectrum was accumulated by using a radioactive source as the start and an oscillator-generated pulse as the stop. This yields a time spectrum in which the time width of each channel is proportional to the number of counts recorded in that channel. An absolute time calibration was achieved by using the beam at

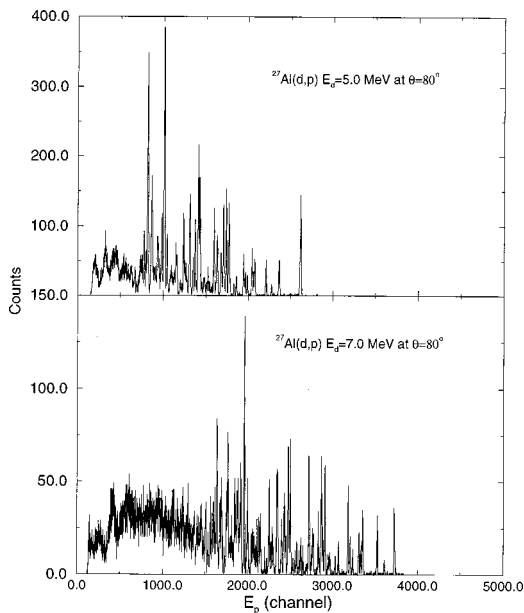


FIG. 2. Typical (d,p) spectra. The data shown are for $^{27}\text{Al}(d,p)$ at 80° .

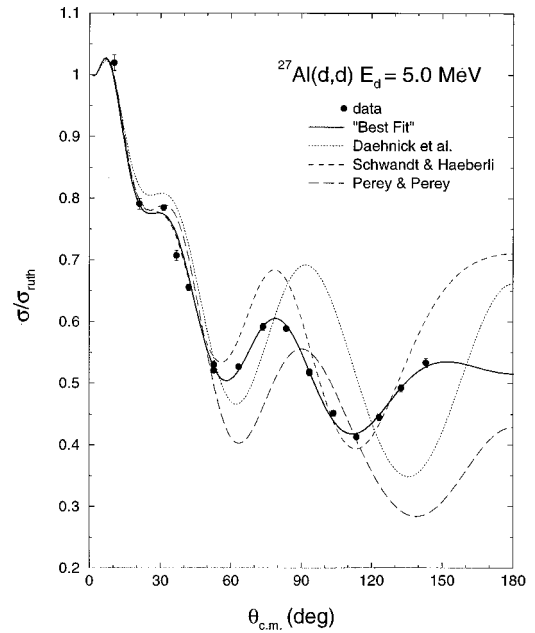


FIG. 3. Elastic scattering angular distribution for Al at 5 MeV. The data represent measured values. Curves shown are for the optical potentials of Perey and Perey, Daehnick *et al.*, and Schwandt and Haeberli. An additional curve represents the best fit obtained from a search.

a repetition rate of 5 MHz to generate gamma rays from the target at intervals of 200 ns but allowing only every sixteenth stop pulse to be registered. This gives 16 calibration peaks spaced at intervals of 200 ns across the spectrum. The combination of these two techniques gives an absolute calibration of the width of each time channel across the spectrum.

The detector efficiency was measured with the use of a neutron “standard” spectrum. A measurement of the neutron spectrum from a stopping target of ^{27}Al bombarded with 7.44 MeV deuterons has been made with a fission chamber at an angle of 120° [1]. The cross section for production of neutrons from 0.2 to 14.5 MeV has been determined to an accuracy of 6%. A measurement of this spectrum with any detector allows it to be calibrated over this energy range.

The elastic scattering measurements were subjected to an optical model analysis. Global optical model parameter sets have been proposed by Perey and Perey [2] and Daehnick *et al.* [3], while Schwandt and Haeberli [4] have derived parameters specifically for aluminum. The latter study did not include data below 7 MeV, however. Values for V and W at 5 MeV were inferred for this potential by extrapolating the behavior observed between 7 and 9 MeV down to 5 MeV.

Figures 3–6 show the comparison of the potentials of Refs. [2–4] with the present data. All of these parameter sets produce fairly good agreement for angles below 50° . This is perhaps not surprising, since the small angle scattering is dominated by Coulomb effects. At larger angles, particularly for aluminum, the predictions tend to go out of phase with one another and with the data.

Fits were carried out with a number of different starting points. No polarization data were included in the fits, so little sensitivity to the spin orbit potential was found. Nearly

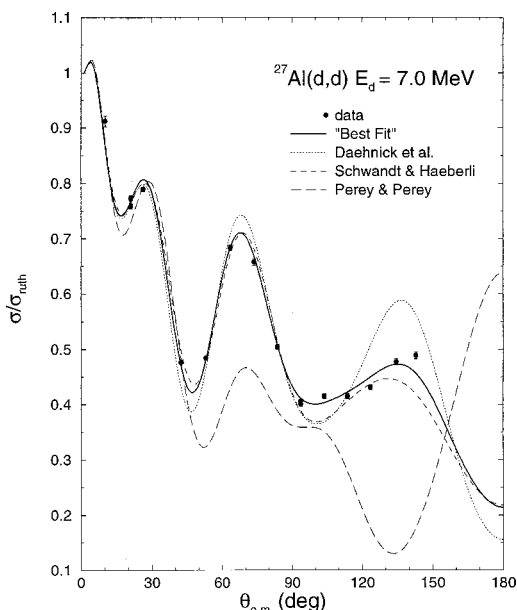


FIG. 4. Same as Fig. 3 for Al at 7 MeV.

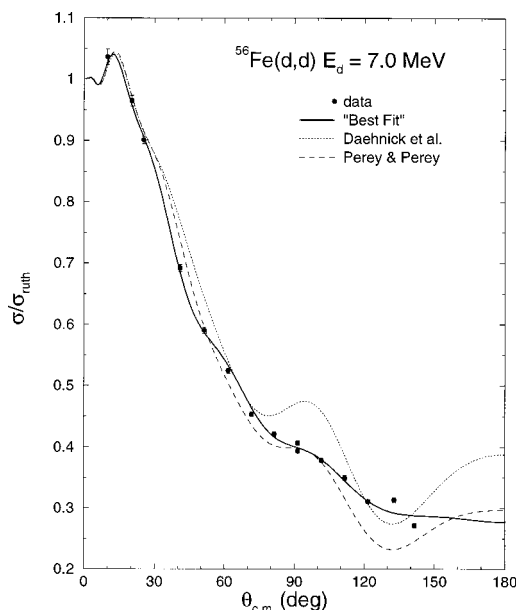


FIG. 6. Same as Fig. 5 for 7 MeV.

equivalent results for the elastic scattering were found using the Schwandt and Haerberli spin orbit potential as with the potential of Daehnick *et al.* Since the purpose of this investigation was not a study of the optical model but rather the determination of the relative importance of direct and compound reactions, we attempted to find how reliably the absorption cross section could be inferred from an optical analysis. To avoid problems with the V_0R^2 ambiguity [5] searches did not allow variation of both of these parameters simultaneously.

Searches were started at the parameter values of Perey and Perey and Daehnick *et al.* for both targets and with those of Schwandt and Haerberli for aluminum. In each case, the

real potential and the imaginary potential were the only parameters varied. The results were much improved χ^2 values in fits to the elastic scattering (usually the improvement was a factor of 4–10) but the absorption cross section changed by less than 10%. To examine the possibility that an alternative geometry would provide a better fit than one of the global geometries, a number of fits were completed using slightly modified geometries. Of these, the one with the smallest χ^2 values is tabulated in Table I for Al and Table II for Fe. In these tables the corresponding parameters for the global potentials are also shown. The best-fit angular distributions are shown in Figs. 3–6.

A comparison of the absorption cross sections predicted by these potentials is presented in Table III. The spread in values obtained from the various fits seems to be consistent with an estimate of 5% for the error on the determination of the absorption cross sections. The average of the absorption cross section obtained with four other fits with similar geometries and the dispersion of the values about these averages is consistent with those tabulated and is about 5%.

The unmodified value of the absorption cross section from Schwandt and Haerberli (SH) potential is close to the final best fit value for this geometry, presumably reflecting the fact that the SH potential was derived for aluminum. The Perey and Perey absorption cross section also changes only slightly, except for aluminum at 7 MeV, where a 5% change is observed. The best fit values with the geometry of Daehnick *et al.* are usually about 20% higher than the original potential strengths gave.

Previous studies of deuteron-induced reactions on these targets give very little guidance on what fraction of the cross section is direct at these energies. A primary problem is that an assessment of the overall fraction requires a complete data set and this is usually not available. Studies of optical model parameters require only elastic scattering data. Thus, most studies of elastic scattering have not included other deuteron-induced reactions. Studies of (d, α) reactions have typically

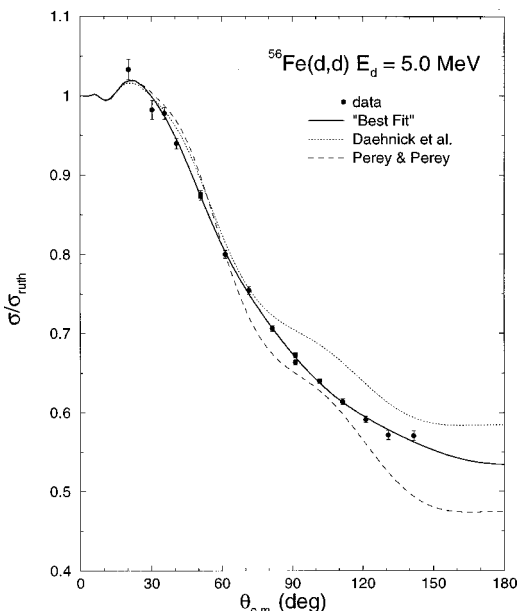


FIG. 5. Same as Fig. 3 for Fe at 5 MeV, except that Schwandt and Haerberli is omitted.

TABLE I. Optical model parameters for Al. W represents a volume absorption term with Woods-Saxon form; W_D is a derivative Woods-Saxon term.

		E (MeV)	V (MeV)	W (MeV)	W_D (MeV)	V_{SO} (MeV)		
Perey and Perey	original	5	88.57		15.6			
	best fit	5	102.3		24.6			
Daehnick <i>et al.</i>	original	5	91.01	0.031	12.3	7.185		
	best fit	5	105.8		14.7	7.185		
Schwandt and Haerberli	original	5	113.7	11.8				
	best fit	5	115.5	14.1				
Best fit		5	113.3		15.76	10.7		
Perey and Perey	original	7	88.13		16.01			
	best fit		96.7		27.6			
Daehnick <i>et al.</i>	original	7	90.49	0.062	12.32	7.127		
	best fit	7	100.8		17.6			
Schwandt and Haerberli	original	7	112.05	14.68		9.0		
	best fit	7	110.2	14.6				
Best fit		7	110.1		16.11	9.0		
		E (MeV)	r (fm)	a (fm)	r_w (fm)	a_w (fm)	r_{SO} (fm)	a_{SO} (fm)
Perey and Perey			5, 7	1.15	0.81	1.34	0.68	
Daehnick <i>et al.</i> 5, 7			1.17	0.72	1.325	0.74	1.07	0.66
Schwandt and Haerberli 7			1.05	0.86	1.573	0.625	0.75	0.4
Best fit 5, 7			1.05	0.86	1.55	0.63	0.75	0.4

not included (d, p) measurements, since the parameters of a ΔE counter used for alpha detection are often different than one would choose for proton detection. Measurements of spectra for the (d, α) reaction on ^{27}Al have been made by

Cassagnou *et al.* [6], Gadioli *et al.* [7], Naqib *et al.* [8], and Bottega *et al.* [9] at energies below 10 MeV and by Liu and Fortune [10] at 12 MeV. In each of these studies, the dominant reaction mechanism was found to be compound nuclear,

TABLE II. Optical model parameters for Fe.

		E (MeV)	V (MeV)	W (MeV)	W_D (MeV)	V_{SO} (MeV)		
Perey and Perey	original	5	93.49		15.6			
	best fit		118.7		34.1			
Daehnick <i>et al.</i>	original	5	93.18	0.031	12.3	7.185		
	best fit		118.2		14.9			
Best fit		5	95.4		14.45	7.19		
Perey and Perey	original	7	93.05		16.01			
	best fit		89.8		20.5			
Daehnick <i>et al.</i>	original	7	92.66	0.062	12.32	7.127		
	best fit		88.7		13.9			
Best fit		7	89.5		14.15	7.13		
		E (MeV)	r (fm)	a (fm)	r_w (fm)	a_w (fm)	r_{SO} (fm)	a_{SO} (fm)
Perey and Perey			5, 7	1.15	0.81	1.34	0.68	
Daehnick <i>et al.</i>			5, 7	1.17	0.72	1.325	0.74	1.07
Best fit			5, 7	1.12	0.86	1.485	0.68	1.07

TABLE III. Deuteron absorption cross sections predicted by various optical potentials.

Nucleus	Energy (MeV)	Perey and Perey		Daehnick <i>et al.</i>		Schwandt		This work (mb)
		orig. (mb)	best fit (mb)	orig. (mb)	best fit (mb)	orig. (mb)	best fit (mb)	
²⁷ Al	5.0	1034	1027	848	1011	1066	1069	1092
	7.0	1202	1267	947	1214	1271	1253	1278
⁵⁶ Fe	5.0	524	596	411	523			561
	7.0	970	968	775	917			1074

though direct amplitudes to some states were observed in Ref. [10]. Cross sections for ²⁷Al(*d,p*) have been measured by Carola and van der Baan [11] at 12 MeV; these authors focused on determining the stripping strength to levels in the lowest few MeV of excitation in ²⁸Al. No effort was made to estimate the fraction of the (*d,p*) cross section which was direct and no measurements were presented of protons at low emission energies. Similar studies [12,13] have been reported for the ²⁷Al(*d,n*) reaction. In both cases, direct reaction analysis was applied to cross sections to the lowest few states. On the other hand, studies at low energy of (*d,p*) [14] and (*d,n*) [15] have found behavior consistent with Ericson fluctuations in the low-lying residual states, indicating that for $E_d < 6$ MeV a substantial compound amplitude is present in the cross section to these states.

The situation for ⁵⁶Fe is fairly similar. Measurements of the (*d,α*) reaction for ⁵⁶Fe have been reported by Majumder *et al.* [16]. Carried out at $E_d = 12$ MeV, this measurement focused on the low-lying levels in ⁵⁴Mn and compared direct calculations with the data. Additional studies of (*d,p*) [17] and (*d,n*) [18] have been reported, but neither of these has measured the entire emission spectrum. A study of ⁵⁶Fe(*d,n*) by Mishra *et al.* [19] comes closest to addressing the question of how much of the reaction cross section corresponds to compound nuclear processes. A comparison of the ⁵⁶Fe(*d,n*) and ⁵⁷Fe(*p,n*) spectra was used to infer the fraction of the deuteron absorption cross section which was compound nuclear. Level density parameters for the ⁵⁷Co nucleus had been deduced from the (*p,n*) spectra. Compound nuclear fractions of about 0.75 were deduced from these data, with the results showing a tendency to increase as the bombarding energy increased. Significant uncertainties were introduced by the fact that the data did not include proton or alpha particle emission spectra and because no measurements of the absorption cross section were made. Thus, the comparison was between measured neutron spectra and calculated (from the optical model with global parameters) absorption cross sections.

Hauser-Feshbach calculations for the two compound nuclei formed in the present experiment were made with the code HF [20]. Optical model parameters for the proton, neutron and α channel were taken from Perey and Perey [2], Rapaport [21], and McFadden and Satchler [22], respectively, while the deuteron parameters were taken from the present data. An initial calculation was made without reducing the transmission coefficients for deuterons in the en-

trance channel. This would only be appropriate if 100% of the absorption processes occurred through formation of a compound nucleus. Although this yielded approximately the correct ratio between neutrons, protons and alphas, the shapes of the spectra were wrong. Although inelastic cross sections for deuterons were measured, the magnitude of the cross sections was less than 2% of the total absorption. The calculations indicated that the compound elastic was a negligible fraction of the observed elastic cross section and the calculated compound nuclear cross sections for deuteron inelastic scattering were also small.

The small binding energy of the deuteron makes both (*d,n*) and (*d,p*) *Q* values positive. At an energy of 2.22 MeV in the center-of-mass system, the deuteron can dissociate, yielding a proton and a neutron, assuming a third body is nearby to provide a momentum balance. This could also occur as the result of deuteron capture by the target to form a compound nucleus, followed by sequential neutron and proton decay. The Hauser-Feshbach calculations, as expected, show the neutron, proton and α as the most important decay channels, in that order, but the *Q* values are such that the (*d,2n*) reaction cannot occur at the present bombarding energies. Further, the (*d,2p*) reaction has a more negative *Q* than the (*d,np*). Thus, the target cross sections at both energies for both targets are calculated to be largest for (*d,np*) and (*d,pn*).

Angular distributions for protons and neutrons showed forward peaking in high-energy bins but very little change in cross section with angle beyond 80°. α particle angular distributions were nearly symmetric. It was, therefore, assumed that a separation of the cross sections into direct and compound parts could be made by reflecting the data points for $\theta > 90^\circ$ about 90° and fitting the symmetric angular distributions which resulted with Legendre polynomials to give an estimate of the compound cross section. These values were then subtracted from the measured cross sections to yield a direct component.

This component has characteristics which are consistent with the identification as direct. A substantial fraction of this cross section is found at high outgoing energies, rather than showing a low-energy peak as the compound portion does. The cross section identified as direct was compared with the absorption cross section to infer a fraction of the reaction cross section corresponding to direct processes. For aluminum, the fraction was 0.2 at 5 MeV and 0.25 at 7 MeV, while for iron it was 0.15 at 5 and 0.3 at 7 MeV. Each of

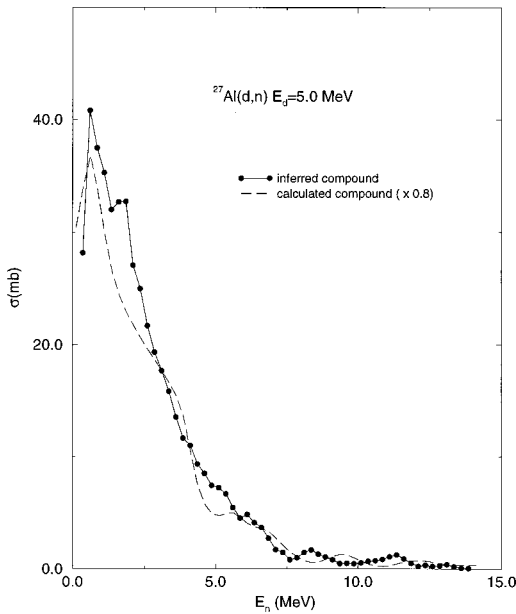


FIG. 7. Cross sections for the $^{27}\text{Al}(d,n)$ reaction at 5 MeV bombarding energy. The dots represent angle integrals calculated as explained in the text. Hauser-Feshbach calculations have been multiplied by the factor of 0.8, which represents the fraction of the absorption cross section which is inferred to be compound.

these numbers is an upper limit, obtained by assuming that no direct processes produce two particles. Inspection of the spectra obtained for the direct reaction portion indicates that about 70–75 % of the particles are emitted with enough energy to preclude emission of a second particle. Thus, these values could be too large by as much as 0.09 (for the 0.3

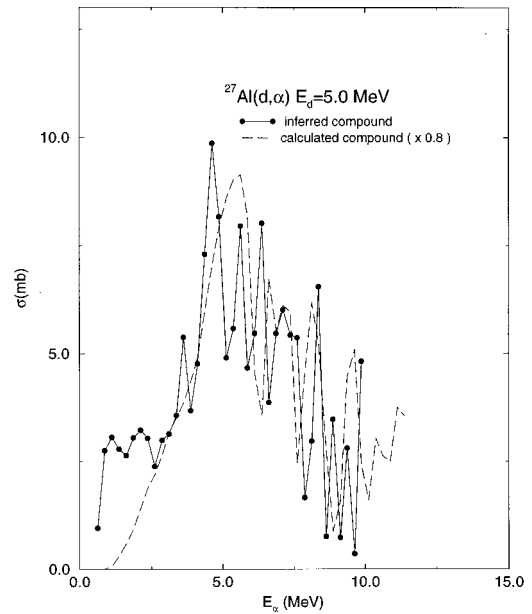


FIG. 9. Cross sections for the $^{27}\text{Al}(d,\alpha)$ reaction at 5 MeV bombarding energy. The dots represent angle integrals calculated as explained in the text. Hauser-Feshbach calculations have been multiplied by the factor of 0.8, which represents the fraction of the absorption cross section which is inferred to be compound.

values) if all of the direct reactions which yield energies allowing the emission of a second particle were to produce such a particle decay in a direct second stage. It is more plausible that a second step would be a compound decay.

An exception to this would be a one-step direct reaction which resulted in the dissociation of the deuteron without

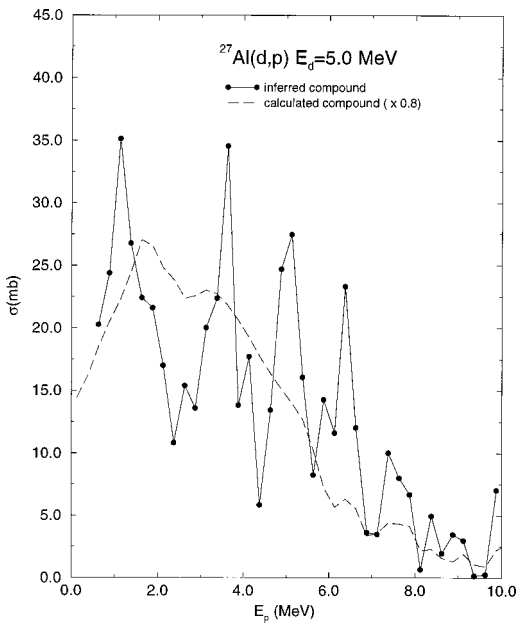


FIG. 8. Cross sections for the $^{27}\text{Al}(d,p)$ reaction at 5 MeV bombarding energy. The dots represent angle integrals calculated as explained in the text. Hauser-Feshbach calculations have been multiplied by the factor of 0.8, which represents the fraction of the absorption cross section which is inferred to be compound.

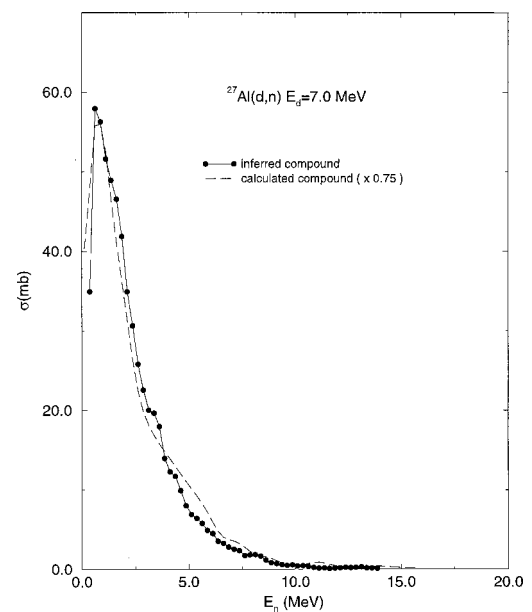


FIG. 10. Cross sections for the $^{27}\text{Al}(d,n)$ reaction at 7 MeV bombarding energy. The dots represent angle integrals calculated as explained in the text. Hauser-Feshbach calculations have been multiplied by the factor of 0.75, which represents the fraction of the absorption cross section which is inferred to be compound.

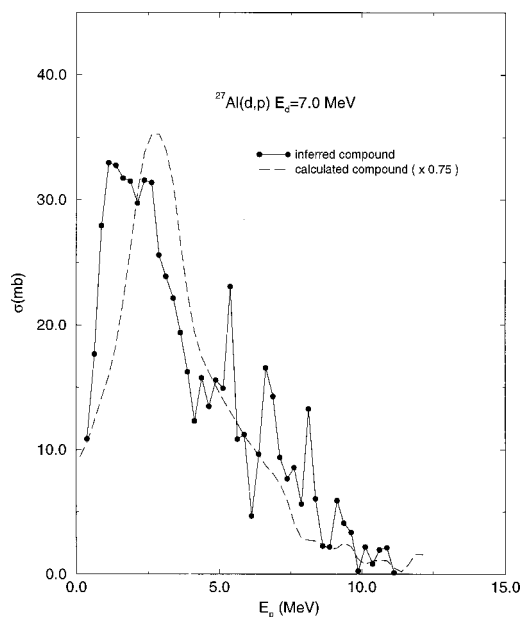


FIG. 11. Cross sections for the $^{27}\text{Al}(d,p)$ reaction at 7 MeV bombarding energy. The dots represent angle integrals calculated as explained in the text. Hauser-Feshbach calculations have been multiplied by the factor of 0.75, which represents the fraction of the absorption cross section which is inferred to be compound.

forming a compound nucleus. These reactions would have the feature that E_p and E_n would sum to the bombarding energy minus 2.2 MeV. At angles about 50° , there are peaks in the neutron and proton spectrum which meet this criterion. These peaks sum to about 15 mb for each target at each energy. A more definitive determination of whether this is

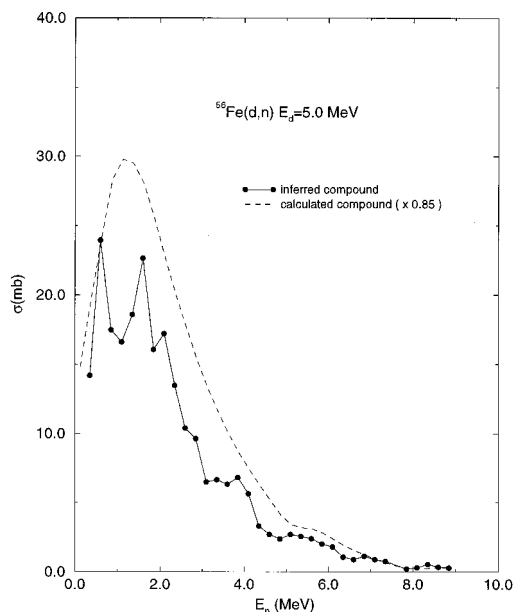


FIG. 13. Cross sections for the $^{56}\text{Fe}(d,n)$ reaction at 5 MeV bombarding energy. The dots represent angle integrals calculated as explained in the text. Hauser-Feshbach calculations have been multiplied by the factor of 0.85, which represents the fraction of the absorption cross section which is inferred to be compound.

the reaction mechanism producing these peaks would require coincidence measurements.

The results of Hauser-Feshbach calculations renormalized by the fraction of reactions which are compound are shown in Figs. 7–18. Level density parameters for the ^{29}Si compound system were taken from Huang *et al.* [23]; level den-

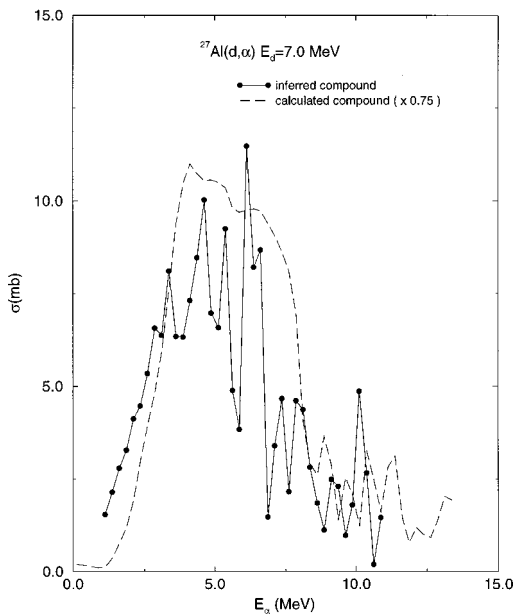


FIG. 12. Cross sections for the $^{27}\text{Al}(d,\alpha)$ reaction at 7 MeV bombarding energy. The dots represent angle integrals calculated as explained in the text. Hauser-Feshbach calculations have been multiplied by the factor of 0.75, which represents the fraction of the absorption cross section which is inferred to be compound.

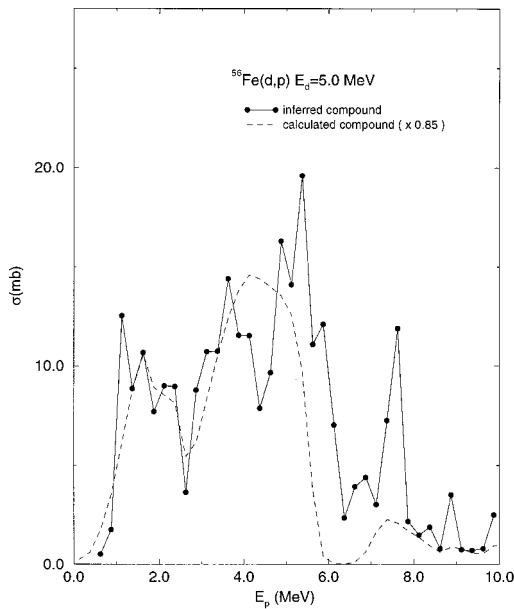


FIG. 14. Cross sections for the $^{56}\text{Fe}(d,p)$ reaction at 5 MeV bombarding energy. The dots represent angle integrals calculated as explained in the text. Hauser-Feshbach calculations have been multiplied by the factor of 0.85, which represents the fraction of the absorption cross section which is inferred to be compound.

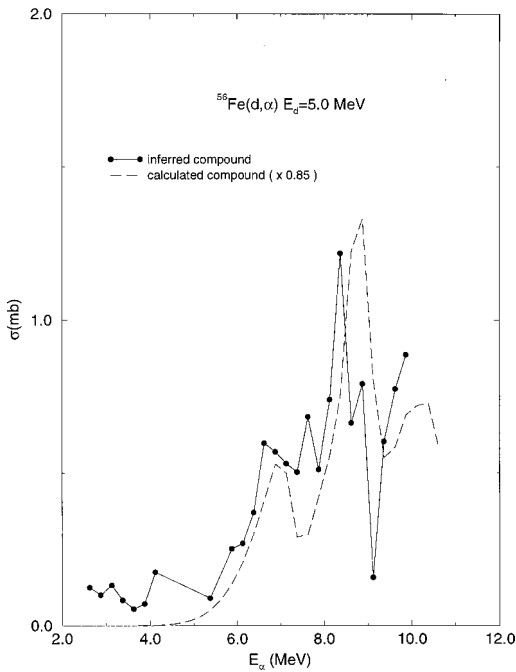


FIG. 15. Cross sections for the $^{56}\text{Fe}(d,\alpha)$ reaction at 5 MeV bombarding energy. The dots represent angle integrals calculated as explained in the text. Hauser-Feshbach calculations have been multiplied by the factor of 0.85, which represents the fraction of the absorption cross section which is inferred to be compound.

sity set *A* produced good agreement with the data. Level density parameters for the ^{58}Co system were taken from Mishra *et al.* [19]. The data represent the angle integrals of the portion of the spectrum inferred to be compound using

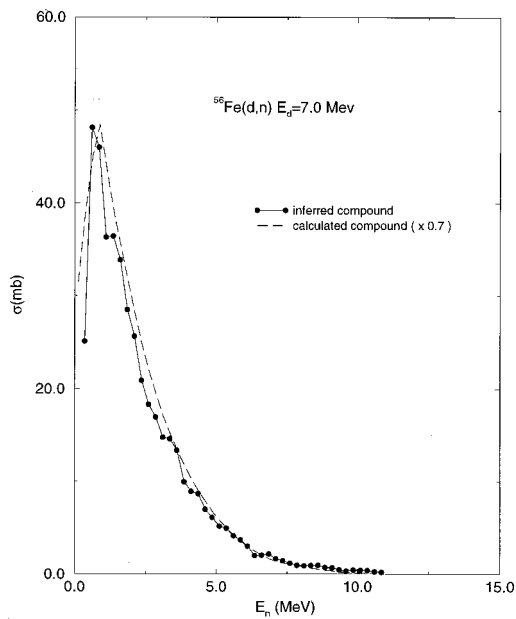


FIG. 16. Cross sections for the $^{56}\text{Fe}(d,n)$ reaction at 7 MeV bombarding energy. The dots represent angle integrals calculated as explained in the text. Hauser-Feshbach calculations have been multiplied by the factor of 0.7, which represents the fraction of the absorption cross section which is inferred to be compound.

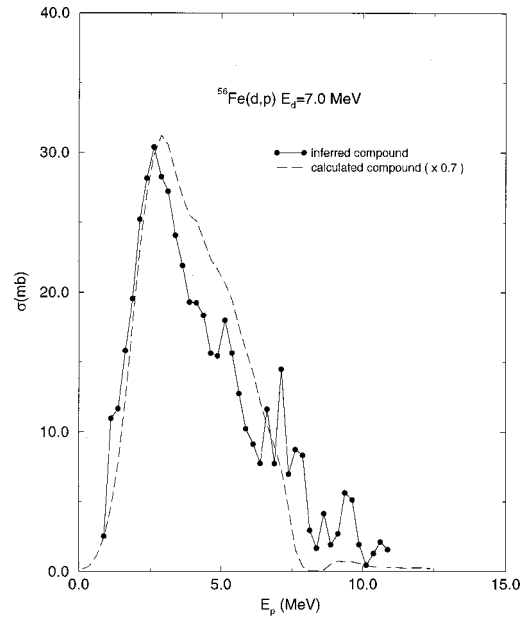


FIG. 17. Cross sections for the $^{56}\text{Fe}(d,p)$ reaction at 7 MeV bombarding energy. The dots represent angle integrals calculated as explained in the text. Hauser-Feshbach calculations have been multiplied by the factor of 0.7, which represents the fraction of the absorption cross section which is inferred to be compound.

the procedure described previously. Good general agreement was found.

The role of isospin [24] in these calculations was also examined. A recent study [25] of (n,p) , (n,d) , and (n,α) reactions on silicon has determined that the primary conse-

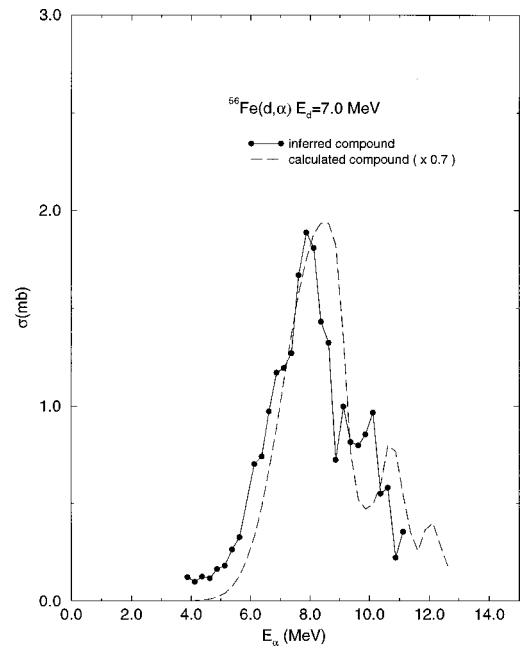


FIG. 18. Cross sections for the $^{56}\text{Fe}(d,\alpha)$ reaction at 7 MeV bombarding energy. The dots represent angle integrals calculated as explained in the text. Hauser-Feshbach calculations have been multiplied by the factor of 0.7, which represents the fraction of the absorption cross section which is inferred to be compound.

quence of isospin is on the α particle yield at energies high enough for second and third stage particle decay. This study is on reactions proceeding through the same compound nucleus (^{29}Si) as the deuteron bombardments of aluminum. Use of the same approach for the present data gives an enhancement of 20% in the α yield for aluminum, but the effects are less than 10% in other channels.

There are three other papers which have results with which the present data can be compared. Mishra *et al.* [19] inferred a value of about 0.75 for the fraction of reactions that are compound nuclear. This result was derived for ^{56}Fe in the energy range of the present measurement. The present results are slightly larger but are in good agreement with the Mishra *et al.* result. Although the Mishra results suggest that the fraction increases slightly with energy, the present results show an opposite trend. West *et al.* [26,27] have studied the same problem on neighboring isotopes at energies above 10 MeV. They find compound nuclear fractions which are about 0.75 at 10 MeV and decrease above this energy. This is also in good agreement with the extrapolation of the present data. The West *et al.* papers rely on radiochemical data and therefore sample a number of final channels but do not have information on channels such as (d,np) which leads to a stable residual nucleus.

Finally, the present results do illustrate the difference between proton- and deuteron-induced reactions at low energy.

A recent paper by Boukharouba *et al.* [28], examined proton-induced reactions on iron isotopes at these energies. They were found to be about 95% compound nuclear.

III. SUMMARY

A study of deuteron-induced reactions on aluminum and iron has yielded elastic (d,p) , (d,α) , and (d,n) cross sections at 5 and 7 MeV. An optical model analysis gives optical model parameters; these yield higher values for the absorption cross section than predicted by one global optical model.

Decomposition of the (d,p) , (d,n) , and (d,α) spectra into components produced by direct and compound reactions give fractions of about 75% for the portion of the absorption cross section produced by compound reactions. Nearly all of the direct cross section produces protons or neutrons, with the alpha spectra showing very small direct components.

ACKNOWLEDGMENTS

This work has been supported by the United States Department of Energy under Grant No. DE-FG02-88ER40387. One of the authors (S.I.A.) acknowledges support received from the King Fahd University of Petroleum and Minerals, Dhahran, Saudi Arabia.

-
- [1] T.N. Massey, S. Al-Quraishi, C.E. Brient, J.F. Guillemette, S.M. Grimes, D. Jacobs, J.E. O'Donnell, J. Oldendick, and R. Wheeler, Nucl. Sci. Eng. **129**, 175 (1998).
- [2] C.M. Perey and F.G. Perey, At. Data Nucl. Data Tables **13**, 293 (1974).
- [3] W.W. Daehnick, J.D. Childs, and Z. Vrcelj, Phys. Rev. C **21**, 2253 (1980).
- [4] P. Schwandt and W. Haerberli, Nucl. Phys. **A110**, 585 (1968).
- [5] P.T. Andrews, R.W. Clift, L.L. Green, J.F. Sharpey-Schafer, and R.N. Maddison, Nucl. Phys. **56**, 422 (1964).
- [6] Y. Cassagnou, C. Levi, M. Mermaz, and L. Papineau, Phys. Lett. **2**, 93 (1962).
- [7] E. Gadioli, G.M. Marazzan, and G. Pappalardo, Phys. Lett. **11**, 130 (1964).
- [8] I.M. Naqib, R. Gleyvod, and N.P. Heydenburg, Nucl. Phys. **66**, 129 (1965).
- [9] A. Bottega, W.R. Murray, and W.J. Naude, Nucl. Phys. **A136**, 265 (1969).
- [10] G.B. Liu and H.T. Fortune, Nucl. Phys. **A496**, 1 (1989).
- [11] T.P.G. Carola and J.G. van der Baan, Nucl. Phys. **A173**, 414 (1971).
- [12] B. Lawergren, G.C. Morrison, and A.T.G. Ferguson, Nucl. Phys. **A106**, 455 (1968).
- [13] W. Bohne, H. Fuchs, K. Grabisch, M. Hagen, H. Homeyer, U. Janetzki, H. Lettau, K.H. Maier, H. Morgenstern, P. Pietrzyk, G. Roschert, and J.A. Scheer, Nucl. Phys. **A131**, 273 (1969).
- [14] M. Corti, M.G. Marazzan, M. Milazzo, and L. Colli Milazzo, Nucl. Phys. **77**, 625 (1966).
- [15] F.B. Bateman, S.M. Grimes, N. Boukharouba, V. Mishra, C.E. Brient, R.S. Pedroni, T.N. Massey, and R.C. Haight, Phys. Rev. C **55**, 133 (1997).
- [16] A.R. Majumder, H.M. Sun Gupta, and A. Guichard, Nucl. Phys. **A209**, 615 (1973).
- [17] A. Sperduto and W.W. Buechner, Phys. Rev. **134**, B142 (1964).
- [18] A. Adam, O. Bersillon, and S. Joly, Phys. Rev. C **14**, 92 (1976).
- [19] V. Mishra, N. Boukharouba, C.E. Brient, S.M. Grimes, and R.S. Pedroni, Phys. Rev. C **49**, 750 (1994).
- [20] S.M. Grimes, J.D. Anderson, J.W. McClure, B.A. Pohl, and C. Wong, Phys. Rev. C **10**, 2373 (1974).
- [21] J. Rapaport, Phys. Rep. **87**, 36 (1982).
- [22] L. McFadden and G.R. Satchler, Nucl. Phys. **84**, 177 (1966).
- [23] Po-lin Huang, S.M. Grimes, and T.N. Massey, Phys. Rev. C **62**, 024002 (2000).
- [24] S.M. Grimes, Phys. Rev. C **46**, 1064 (1992).
- [25] F.B. Bateman, R.C. Haight, M.B. Chadwick, S.M. Sterbenz, S.M. Grimes, and H. Vonach, Phys. Rev. C **60**, 064609 (1999).
- [26] H.I. West, Jr., M.G. Mustafa, R.G. Lanier, and H. O'Brien, Phys. Rev. C **43**, 1352 (1991).
- [27] H.I. West, Jr., R.G. Lanier, and M.G. Mustafa, Phys. Rev. C **35**, 2067 (1987).
- [28] N. Boukharouba, C.E. Brient, S.M. Grimes, V. Mishra, and R.S. Pedroni, Phys. Rev. C **46**, 2375 (1992).